

SUPPORTING MATERIAL:

Cell-to-cell diversity as revealed by single cell analysis performed with a synchronous *Chlamydomonas* culture

Andreas Garz,[†] Michael Sandmann,[‡] Michael Rading,[§] Sascha Ramm,[‡] Ralf Menzel,[†] and Martin Steup^{‡*}

[†]Institute of Physics and Astronomy, Department of Photonic; [‡]Institute of Biochemistry and Biology, Department of Plant Physiology, University of Potsdam, Karl-Liebknecht-Str. 24-25, 14476 Potsdam-Golm, Germany; [§]Max-Planck-Institute of Colloids and Surfaces, Department of Theory and Biosystems, Am Mühlenberg 1, 14476 Potsdam-Golm, Germany

1. GROWTH CONDITIONS OF THE ALGAL CELLS

2. INFLUENCE OF BIREFRINGENCE

3. SUPPORTING TABLES

Table S1: SPEARMAN RANK CORRELATION COEFFICIENT

Table S2: PARAMETER MEAN VALUE AND WIDTH (2σ) OF VOLUME DISTRIBUTION

Table S3: PARAMETER MEAN VALUE AND WIDTH (2σ) OF CELLULAR STARCH DENSITY

4. SUPPORTING FIGURES

Fig. S1: SHG signal obtained from a BBO crystal

Fig. S2: Optical device

Fig. S3: Single cell analyses following the DARK-induced starch degradation

Fig. S4: High resolution image of the starch-derived SHG signal from a single cell

Fig. S5: High resolution image of the starch-derived SHG signal from a single cell

SUPPORTING MATERIAL

1. GROWTH CONDITIONS OF THE ALGAL CELLS

For synchronization, aliquots of the preculture were transferred into a synthetic nutrient medium whose five macrocompounds are described by (1). Microelements were applied according to (2). However, the concentration of all microelements was reduced to 50 % of the original version. In freshly prepared nutrient medium the pH value is 7.35.

For synchronization under axenic conditions, cells were kept at 34°C in a 12 h light/12 h dark regime (standard conditions). Cells were grown in glass tubes (3.5 cm inner diameter, 45 cm length, maximal culture volume 300 ml) placed in a thermostat similar to that described in (2). However, glass tubes were illuminated from both the front and back side using 6 fluorescent tubes each (3 tubes each Osram of T8 L 18W/840 LUMILUX Cool White G13 and Osram L 18W/77 FLUORA G13). After 6 months, all tubes were replaced by new ones. Illumination was measured inside the *Chlamydomonas* suspension using a Radiometer (Quantum Scalar Laboratory Type QSL-2100; Biospherical Instruments Inc., San Diego, USA). Inside the cell suspension (standard conditions), illumination is approximately 900 and 550 $\mu\text{mol photons m}^{-2} \text{s}^{-1}$ at the beginning and the end of the light period, respectively.

Cells were continuously agitated by aeration with air supplemented with 2 % [v/v] CO_2 (2). At the end of the dark period, the suspension was diluted to 7×10^5 cells ml^{-1} using fresh nutrient medium (standard conditions). Cells were fully synchronized after four light-dark cycles and daily dilution. Synchrony was maintained for an unlimited number of cycles but all experiments presented here were performed one day after synchronization was achieved.

2. INFLUENCE OF BIREFRINGENCE

Birefringence: Anisotropic matter exhibit two or more refractive indices of light dependent on polarisation or direction of incoming light. In the simplest case birefringence is defined as:

$$\text{Birefringence } (B) = |n_e - n_o| \quad (1)$$

Here n is the refractive index. Subscript e stands for the extraordinary and o for the ordinary ray as they emerge from an anisotropic material, such as starch.

Following a classical optical concept, the value of birefringence can be quantified given by the optical path difference (Γ).

$$\Gamma = (n_e - n_o) \cdot d \quad (2)$$

Where d is the specimen thickness till which birefringence is negligible. Under the assumption of a noncritical optical path difference of $\lambda/10 = 80 \text{ nm}$ and a difference of the refraction indices $|n_e - n_o| = 0.0106$ to 0.0080 (3) the thickness of d ranges from 7.5 to 10 μm .

The calculation was verified by the following experiment: The SHG signal of a Beta-Bariumborat (BBO) crystal was measured in dependence of the penetration depth of the circular polarised light (Fig S1). The crystal was 2 mm thick with a difference of refractive indices of 0.115, which was significantly higher than that of starch. However, according to equation (2), the thickness resulted in $d = 0.7 \mu\text{m}$. Fig. S1 shows the experimental SHG signal depending on the penetration depth of the light. At the z-position of about 25 μm the focal volume started to penetrate the crystal. At about 20 μm the total focal volume was inside the crystal and the maximum SHG intensity was reached. From this point, an acceptable tolerance of 5 % was assumed. Accordingly, a maximum thickness of $d = 0.9 \mu\text{m}$ was obtained. Thus for the BBO crystal, the maximum propagation depth of the incoming light without a significant decrease in the SHG signal is 0.9 μm . This is in good agreement with the theoretical value.

In addition, the same procedure was applied to different starch species (Merck, Sigma, native potato starch). Due to the heterogeneity in size, the maximum thickness ranged from $d = 8$ to 15 μm .

It should be noted, that in a *Chlamydomonas* cell the total starch volume reaches only a maximum of 30 % of the total cell volume. Furthermore, the individual granules are small (two magnitudes lower than the cell volume) and distributed in the cell. Thus, the values obtained above are based on a worst case scenario, since the cellular starch occurs at many subcellular sites each of which is designed as granulum. In practice, the laser light of a high-numerical aperture objective most likely transmits unhampered. Finally, we were able to show in high resolution scans of single cells (Fig. S4 and S5) that no significant influence of the SHG signal occurred depending on penetration depth of the laser light.

In summary, under the conditions used a cell diameter of at least 20 μm is not critical for quantitative starch analysis.

3. SUPPORTING TABLES

Table S1: SPEARMAN RANK CORRELATION COEFFICIENT

Sample	Synth.	Degrad. 1	Degrad. 2	Degrad. 3	Degrad. 4
0h	0.30				
2h	0.12				
4h	0.08				
6h		0.13	0.28	0.09	0.33
6h + 1h		0.14	0.20	0.34	0.25
6h + 2h		0.15	0.15	0.20	0.20
6h + 3h		0.25	0.27	0.25	0.31

Table S1A

Sample	Synth.	Degrad. 1	Degrad. 2	Degrad. 3	Degrad. 4
0h	- 0.39				
2h	- 0.54				
4h	- 0.56				
6h		- 0.48	- 0.54	- 0.49	- 0.50
6h + 1h		- 0.37	- 0.62	- 0.44	- 0.55
6h + 2h		- 0.37	- 0.67	- 0.45	- 0.52
6h + 3h		- 0.23	- 0.58	- 0.50	- 0.63

Table S1B

Table S1. A: Correlation between the Relative Cellular Starch Content (RCSC), as measured by the SHG signal intensities, and the cellular volume (procedure B). **B:** Correlation between the Cellular Starch Density (CSD), as measured by the SHG signal intensities, and the cellular volume; procedure B) based on the cellular volume.

Sample 1 and 2: Starch degradation induced by darkness; sample 3 and 4: Starch degradation induced by DCMU; A 95% confidence interval for mean value and width is given.

Table S2: PARAMETER MEAN VALUE AND WIDTH (2σ) OF VOLUME DISTRIBUTION

Sample	Time	Mean v. [μm^3]	Width (2σ) [μm^3]
Synthes.	0h	114.32 \pm 2.5	96.66 \pm 5.4
	2h	191.39 \pm 8.7	122.83 \pm 16.43
	4h	339.31 \pm 13.5	223.51 \pm 25.73
Degrad. 1	6h	586.29 \pm 16.9	432.22 \pm 33.53
	6h + 1h	568.56 \pm 10.42	438.21 \pm 20.98
	6h + 2h	568.14 \pm 21.92	437.41 \pm 44.13
	6h + 3h	569.00 \pm 14.66	439.42 \pm 29.54
Degrad. 2	6h	567.63 \pm 15.89	428.84 \pm 31.90
	6h + 1h	568.44 \pm 12.88	432.89 \pm 25.81
	6h + 2h	570.18 \pm 15.37	435.85 \pm 30.85
	6h + 3h	568.78 \pm 17.90	440.72 \pm 36.11
Degrad. 3	6h	569.78 \pm 16.43	436.27 \pm 32.30
	6h + 1h	567.91 \pm 15.24	435.16 \pm 30.62
	6h + 2h	569.44 \pm 18.62	439.94 \pm 37.52
	6h + 3h	569.27 \pm 10.49	436.80 \pm 21.07
Degrad. 4	6h	569.71 \pm 16.39	482.25 \pm 34.25
	6h + 1h	569.33 \pm 19.15	434.62 \pm 38.42
	6h + 2h	569.37 \pm 31.32	437.38 \pm 63.04
	6h + 3h	569.83 \pm 10.93	436.30 \pm 21.93

Table S2: Mean value and width (2σ) of volume distribution during starch synthesis (time 0-6 h) and degradation. Sample numbers are defined in Table S2. During cell growth the mean value of volume distribution increases, while the width is broadened. Contrarily, the volume distribution remains the same during induced starch degradation.

Table S3: PARAMETER MEAN VALUE AND WIDTH (2σ) OF CELLULAR STARCH DENSITY (CSD)

Sample	Time	Mean v. [a.u.]	Width (2σ) [a.u.]
Synthes.	0h	2.34 \pm 0.08	2.98 \pm 0.2
	2h	4.22 \pm 0.32	4.31 \pm 0.7
	4h	10.23 \pm 0.67	10.44 \pm 1.5
Degrad. 1	6h	15.92 \pm 0.82	19.72 \pm 2.08
	6h + 1h	14.63 \pm 0.60	23.30 \pm 1.77
	6h + 2h	13.11 \pm 1.02	19.03 \pm 2.85
	6h + 3h	12.37 \pm 0.58	16.24 \pm 1.51
Degrad. 2	6h	16.33 \pm 0.54	14.25 \pm 1.1
	6h + 1h	14.99 \pm 0.42	13.73 \pm 0.9
	6h + 2h	13.07 \pm 0.48	13.17 \pm 1.1
	6h + 3h	11.66 \pm 0.42	10.17 \pm 0.9
Degrad. 3	6h	15.83 \pm 0.78	19.38 \pm 1.94
	6h + 1h	13.70 \pm 0.46	12.90 \pm 1.02
	6h + 2h	11.10 \pm 0.55	12.44 \pm 1.32
	6h + 3h	8.70 \pm 0.21	8.69 \pm 0.49
Degrad. 4	6h	16.31 \pm 0.78	15.50 \pm 1.2
	6h + 1h	13.53 \pm 0.58	12.74 \pm 1.3
	6h + 2h	10.73 \pm 0.77	10.48 \pm 1.7
	6h + 3h	8.32 \pm 0.17	6.71 \pm 0.3

Table S3: Mean value and width (2σ) of cellular starch density (CSD) distribution during starch synthesis (time 0-6 h) and degradation. Sample numbers are defined in Table S2. The mean value of CSD distribution increases during cell growth, while the width is broadened. By contrast, during starch degradation the CSD distribution shifts to lower values and the width decreases.

4. SUPPORTING FIGURES

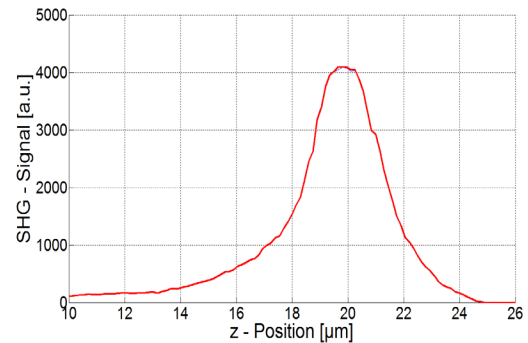


Fig. S1: SHG signal obtained from a BBO crystal

Shown is the SHG signal depending on penetration depth (z-position) of the circular polarised light. At the position of 25 μm lies the air-crystal boundary.

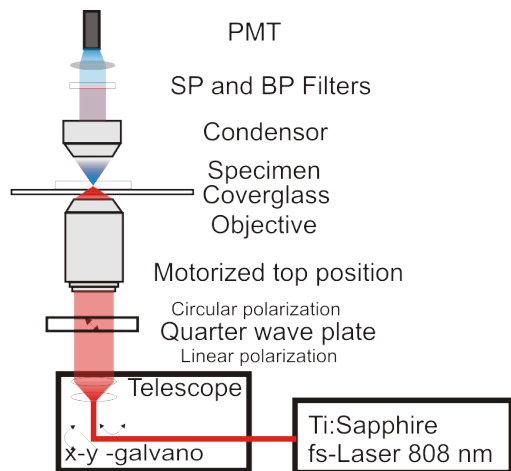


Fig. S2: Optical device.

The laser emits femtosecond pulses at 808 nm with a pulse width of 120 fs and a repetition rate of 80 MHz. X-y-galvano mirrors deflect the beam which is then expanded by a telescope. A quarter wave plate converts the linear polarization of the light into circular polarization. In axial direction, focal position can be adjusted by a motorized objective revolver. The specimen, covered with water, is held on a coverglass. Behind the specimen the SHG light is collected by a condenser. The SHG light, detected by a photomultiplier tube (PMT), is separated from the incoming laser light by using spectral filters.

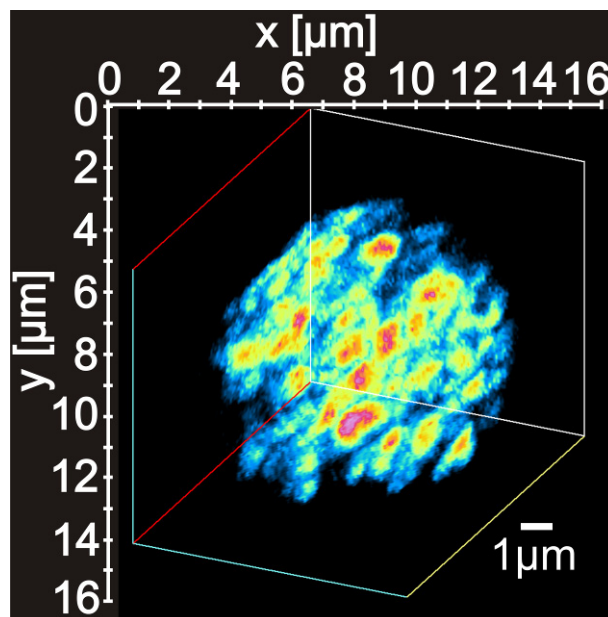


Fig. S4: High resolution image of the starch-derived SHG signal from a single cell

SHG signal intensities from a single cell (false color imaging). Red color: High signal intensity indicating high starch amount; blue color low signal intensity (low starch amount). The cell was taken from a synchronized culture after six hours illumination.

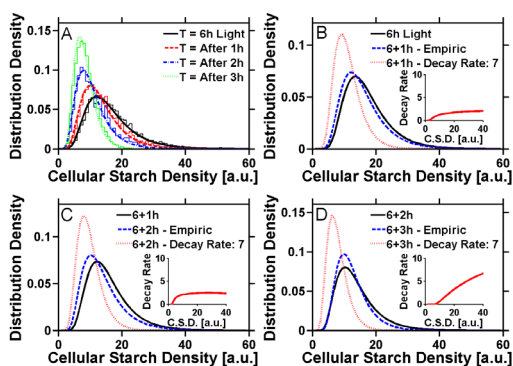


Fig. S3: Single cell analyses following the DARK-induced starch degradation.

A: Probability Density Function of the Cellular Starch Density (CSD) during starch degradation exhibits a lognormal distribution. Unlike starch accumulation, the mean value decreases with time and a more narrow distribution is observed.

B to D: Theoretical and empirical analyses after 1 (B), 2 (C) and 3 (D) h of starch degradation. CSD at the onset of the degradation (i.e. after 6 h illumination) is given in black. Red: distribution obtained by eq. (3) assuming a constant degradation rate. Blue: distribution obtained using the degradation rate calculated for each interval (see insert).

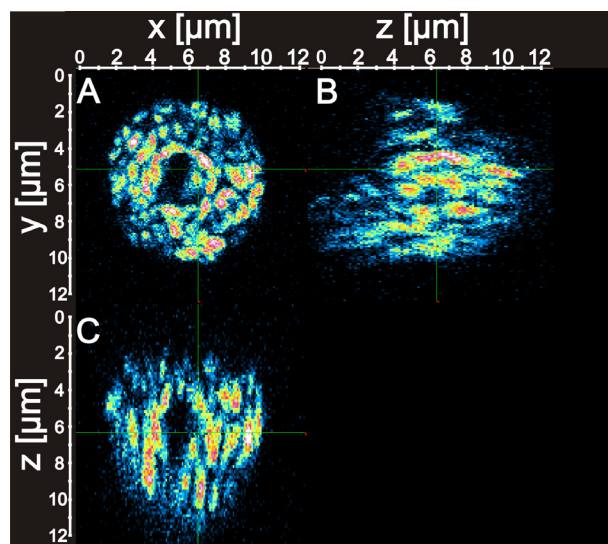


Fig. S5: High resolution image of the starch-derived SHG signal from a single cell

The same cell and colors as in Fig. S4 (A) cross section (x-y-plane) (B) and (C) projection in z-direction No significant signal losses with increasing penetration deep of the laser are noticeable.

SUPPORTING REFERENCES

1. Sueoka, N. 1960. Mitotic replication of deoxyribonucleic acid in *Chlamydomonas reinhardtii*. Proc. Natl. Acad. Sci. U. S. A. 46:83-91.
2. Kuhl, A., and H. Lorenzen. 1964. Handling and culturing of *Chlorella*. In *Methods in cell physiology*. D. M. Prescott, editor. Academic Press. 465:159 - 166.
3. Wolf, M. J., M. M. Macmasters, and V. J. Ruggles. 1962. Refractive indices of wheat starch granules at various moisture levels determined with an interference microscope. *Bioch. et Biophys. Acta* 57:135-142.